Mon. Not. R. Astron. Soc. **000**, 1–6 (2015) Printed 24 April 2015 (MN LATEX style file v2.2)

Evidence for changes in the radiative efficiency of transient black hole X-ray binaries

A. J. Eckersall[1⋆], S. Vaughan[1], G. A. Wynn[1]
[1]*Department of Physics and Astronomy, University of Leicester, Leicester, LE1 7RH, UK*

Draft 24 April 2015

ABSTRACT

We have used pointed *RXTE* data to examine the long-term X-ray light curves of six transient black hole X-ray binaries during their decay from outburst to quiescence. In most cases, there is a period of exponential decay as the source approaches the soft- to hard- state transition, and another period of exponential decay following this transition as the source decays in the hard state. The e-folding times change around the time of the state transition, from typically ≈ 12 d at the end of the soft state to ≈ 7 d at the beginning of the hard state. This factor ~ 2 change in the decay time-scale is expected if there is a change from radiatively efficient emission in the soft state to radiatively inefficient emission in the hard state, overlying an exponential decay in the mass accretion rate. This adds support to the idea that the X-ray emitting region is governed by radiatively inefficient accretion (such as an advection-dominated or jet-dominated accretion flow) during the fading hard state.

Key words: accretion, accretion discs – black hole physics – X-rays: binaries

1 INTRODUCTION

Low-mass X-ray binaries (LMXBs) comprise a black hole (BH) or neutron star (NS), often called the primary, that accretes gas from a secondary star (also called the companion, or donor) with a mass $M_2 \lesssim 1.5\,\mathrm{M}_\odot$. An accretion disc is formed around the BH when the secondary fills its Roche lobe and material passes towards the BH (Shakura & Sunyaev 1973; McClintock & Remillard 2006; Done et al. 2007). In this paper, we concentrate on LMXBs with a BH primary; these systems are powerful but transient sources of X-rays. They spend most of their time in quiescence, with very low luminosity in X-rays and other wavebands, interrupted by outbursts that usually last for weeks–months during which the X-ray luminosity can be comparable to the Eddington luminosity $L_{\rm Edd}$ ($\sim 10^{38} M_{\rm BH}/\,\mathrm{M}_\odot$ erg s^{-1}).

The current explanation for the outburst cycle is based on the disc instability model (DIM; e.g. van Paradijs 1996; King & Ritter 1998; Dubus et al. 2001; Lasota 2001). In the quiescent state, the accretion disc gas is mostly neutral and has a low viscosity. The rate at which mass is transferred from the secondary to the disc is typically larger than mass accretion rate through the disc on to the BH, such that the disc mass and temperature increase over time. As the temperature approaches $\sim 10^4$ K hydrogen ionization causes a dramatic change in the opacity of the gas within the disc that is associated with an increase in the disc viscosity. This triggers an increase in the accretion rate on to the primary, causing an outburst. During the outburst, the disc (and related corona/jet) is a powerful source of X-rays. These X-rays irradiate the accretion disc and raise its temperature above that expected from viscous heating alone, keeping the disc in the hot, high-viscosity phase. Nevertheless, eventually the mass accretion rate will drop, reducing the level of X-ray irradiation and allowing the disc to return to its cool, low-viscosity state. At this point the source returns to quiescence.

One of the generic predictions of the DIM, after inclusion of X-irradiation of the outer disc, is a period of exponential decay in the mass accretion rate: $\dot{M} \propto \exp(-t/\tau_{\rm m})$ (King & Ritter 1998; Dubus et al. 2001; Lasota 2001). The duration and e-folding time $\tau_{\rm m}$ is controlled by system parameters (such as the disc size). Such exponential decays have been observed in several XRB outbursts (Chen et al. 1997; Kuulkers 1998; Jonker et al. 2010; Stiele et al. 2012; Tomsick et al. 2014), although often the decays are interrupted by flares and other re-brightening events.

Within each outburst, XRBs usually show several distinct 'states' characterized by particular X-ray spectral and timing behaviour, but also correlated with other behaviour such as radio emission (e.g. Remillard & McClintock 2006; Done et al. 2007; Belloni 2010). The two most commonly observed states are the *soft* state and the *hard* state. The soft state (sometimes known as the thermal-dominated state) is generally seen near the peak of the outburst and is characterized by an X-ray spectrum dominated by thermal emission from the accretion disc with a temperature $T_{\rm peak} \sim 1$ keV (Remillard & McClintock 2006), and a weak, non-thermal tail of emission to higher energies. The soft state shows only weak rapid X-ray variability and weak, if any, radio emission (Fender et al. 2009). The X-ray emission is powered by a luminous, radiatively efficient accretion disc that is assumed to extend in to the innermost stable circular orbit ($r_{\rm ISCO} = 6r_{\rm g}$ for a non-rotating BH, where the gravitational radius is $r_{\rm g} = GM/c^2$). By radiative

⋆ aje16@le.ac.uk

efficiency we mean the fraction of the accreting mass converted to escaping radiation, $\eta = L_{\rm bol}/\dot{M}c^2$. The hard state – always seen during the rise to outburst and decay to quiescence, and sometimes near outbursts peak – is characterized by an X-ray spectrum dominated by a non-thermal (power law) component, extending up to energies ~ 100 keV, with a much weaker, cooler thermal component ($T_{\rm peak} \lesssim 0.3$ keV) sometimes detectable at lower energies (Remillard & McClintock 2006). The radio and timing properties are also different: the hard state shows strong, rapid X-ray variability (van der Klis 2006; Belloni 2010) and persistent (flat spectrum) radio emission (Fender et al. 2009). The source of the non-thermal emission is not fully understood but is often thought to be the result of either inverse-Compton scattering (of soft photons emitted from the accretion disc) in a corona of hot electrons above the disc (Haardt & Maraschi 1993; Dove et al. 1997; Poutanen 1998), or synchrotron and self-Compton emission produced in the base of the radio jet (Markoff et al. 2001, 2005). There are also intermediate states; these are usually short-lived and occur during transitions between the longer lived hard and soft states (Belloni 2010). It remains an open question how these bright states are related to the quiescent state (Fender et al. 2003; Miller-Jones et al. 2011; Plotkin et al. 2013; Fender & Gallo 2014; Reynolds et al. 2014)

Two varieties of accretion flow models, with distinct X-ray emission mechanisms, are often used to explain the differences between the soft and hard states. One is the standard, optically thick and geometrically thin accretion disc with its strong thermal emission (Shakura & Sunyaev 1973). This disc (when extending down to $r_{\rm ISCO}$) produces the thermal emission that dominates the X-ray spectrum and is assumed to have a high radiative efficiency ($\eta \sim 0.1$, Shakura & Sunyaev 1973) that is approximately constant with accretion rate. We therefore expect a linear scaling between X-ray luminosity and mass accretion rate, $L_{\rm X} \propto \eta\dot{M} \propto \dot{M}$, at least in the regime where $\dot{M}$ is high enough to maintain a such a disc. The other type of accretion flow is any of a group of alternatives to the optically thick accretion disc. Examples of these are the advection dominated accretion flow (ADAF; Narayan & Yi 1995) and the jet-dominated accretion flow (JDAF; Falcke et al. 2004). These are optically thin and generate X-rays via Comptonization, bremsstrahlung and/or cyclo-synchrotron. In the non-thermal-dominated hard states the inner accretion disc may be replaced by this optically thin flow (e.g. Esin et al. 1997) which has a lower radiative efficiency that depends on the accretion rate, e.g. $\eta \propto \dot{M}$. This leads to a non-linear scaling of X-ray luminosity with accretion rate: $L_{\rm X} \propto \eta\dot{M} \propto \dot{M}^2$ (Narayan & Yi 1995). See e.g. Fender et al. (2003), Merloni et al. (2003), Körding et al. (2006) and Coriat et al. (2011) for further discussion of the link between X-ray and radio luminosities, accretion rate and radiative efficiency.

Knevitt et al. (2014) studied the difference in the period distribution of the known LMXBs with NS and BH primaries. They found a dearth of very short period BH systems relative to NS systems that could be reproduced if the BH systems are radiatively inefficient below some critical mass accretion rate. Shorter period binaries have a lower maximum luminosity and may be radiatively inefficient through a substantial fraction of their outbursts. Knevitt et al. (2014) compared different models for the switch between efficient and inefficient accretion and found that only a dramatic change, to an efficiency scaling $\eta \propto \dot{M}^{\beta}$ with $\beta \gtrsim 3$, could explain the observed lack of short-period BH systems.

When the mass accretion rate is decaying exponentially, and the emission is dominated by a radiatively efficient accretion disc, the X-ray luminosity should decay with the same e-folding time: $L_{\rm X} \propto \dot{M} \propto \exp(-t/\tau_{\rm m})$. If the emission is dominated by a radiatively inefficient flow, the X-ray luminosity will decay faster, e.g. for $\eta \propto \dot{M}$ we will have $L_{\rm X} \propto \dot{M}^2 \propto \exp(-2t/\tau_{\rm m})$. The e-folding time of the luminosity is shorter (e.g. $\tau_{\rm m}/2$). Therefore, as discussed in Homan et al. (2005), if there is a change from a radiatively efficient to a radiatively inefficient accretion regime during the period of exponential decay in the mass accretion rate, there should be a decrease in the e-folding time of the X-ray luminosity during the decay. In this paper, we test this hypothesis using some of the best *RXTE* monitoring data of XRB outbursts.

2 OBSERVATIONS AND DATA REDUCTION

2.1 Sample definition

The sample of XRB outbursts is shown in Table 1. We selected all the confirmed and candidate transient BH XRBs listed in Remillard & McClintock (2006). For each one we, identified all the long (>few days) outbursts based on daily light curves of each source from the *RXTE* All-Sky Monitor, and where possible also used data from the *Swift* Burst Alert Telescope, and *MAXI* (Monitor of All-Sky X-ray Image) Gas Slit Camera. These data alone were insufficient to accurately define the decay rates. We therefore selected the subset of outbursts with a sufficient number (> 20) of pointed *RXTE* observations to estimate decay rates in both soft and hard states.

2.2 *RXTE* observations

For each selected outburst we extracted pointed *RXTE* data from the High Energy Astrophysics Science Archive Research Center (HEASARC) archive. We only took data from the Proportional Counter Array (PCA) instrument, in the `STANDARD2` mode which has 129 energy channels. We extracted both source and background spectra for each observation, along with spectral response files using the standard *RXTE* software HEASOFT v6.15.1), and then computed background-subtracted count rates in three energy bands: A = channels 4-44 ($\approx$ 3-20 keV), B = channels 4-10 ($\approx$ 3-6 keV) and C = channels 11-20 ($\approx$ 6-10 keV), as in Motta et al. (2012). The background is obtained using models as *RXTE*/PCA background cannot be measured. We used the hardness ratio $H = C/B$ (Homan & Belloni 2005). Using these we produced light curves, hardness ratio curves and hardness intensity diagrams (HIDs; Belloni et al. 2005) for each outburst. Fig. 1 shows the data for the intensively observed 2005 outburst of GRO J1655−40.

At low count rates (< 10 ct s^{-1}), the data could be affected by systematic errors in the background subtraction and by contaminating sources in the PCA field of view, including diffuse Galactic emission. This often makes the decays appear to slow down towards quiescence (e.g. Homan et al. 2005; Jonker et al. 2010). For each count rate, we computed errors based on standard Poisson statistics. However, these usually underestimate the random scatter in the light curves, as the dominant source of variance is systematic, not random, e.g. the intrinsic, rapid variability of the sources (particularly strong in the hard states) and systematic errors resulting from subtraction of the instrumental background (a more significant effect at low fluxes). As a way to assign similar statistical weight to data points that may differ in flux by two to three orders of magnitude, we assumed 3% errors for all count rates, in both soft and hard states. Thus, a fit is considered 'good' if the model matches to within ~ 3 per cent for most data points.

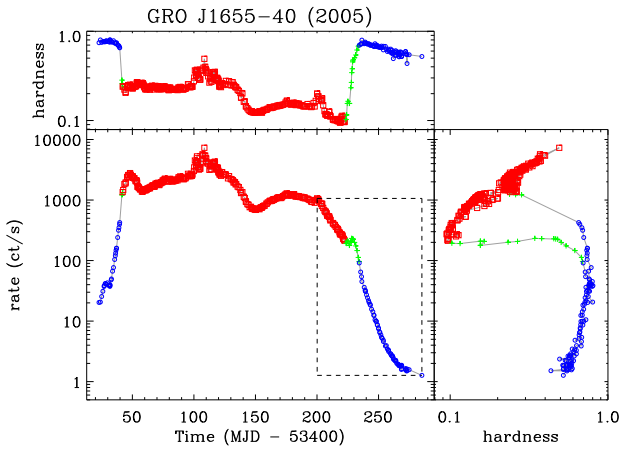

Figure 1. *RXTE* light curve in the $\approx 3-20$ keV band showing the full 2005 outburst of GRO J1655−40, along with a HID (right-hand panel) and hardness ratio curve (top panel). The plot has been coloured to show the spectral states of the source as the outburst progresses: blue circles for the hard state, green crosses for intermediate and red squares for soft. The dashed lines highlight the region shown in Fig. 2.

2.3 *Swift* Observations

We have also made use of *Swift* X-ray Telescope (XRT) observations to track the outburst of GRO J1655−40 to lower count rates than is possible using only the *RXTE* PCA data. As the XRT is an imaging telescope, it is less sensitive to background issues, so we use it to verify our *RXTE* background subtraction. Of our sample only GRO J1655−40 has any useful observations. There are six *Swift* observations during the hard-state decay: three just after the end of the state transition back into the hard state at around MJD 53640, and three a few weeks later at around MJD 53665. The *Swift* XRT data were reduced using HEASOFT v6.15.1. Photon event lists and exposure maps were produced using XRTPIPELINE v0.13.1. For each observation, a source spectrum was extracted from photons in a circular extraction region of radius 30 arcsec, and a background spectrum was extracted from a source-free region of the same image. Response matrix files were generated using XRTMKARF v0.6.1.

The energy bandpass and response of the *Swift* XRT differs and *RXTE* PCA, and so we converted the *Swift* data to equivalent PCA rates for comparison with the *RXTE* monitoring data. We used XSPEC v12.8.2 (Arnaud 1996) to fit a model to the *Swift* XRT spectrum for each observation. The model comprised a blackbody plus power law, all modified by neutral absorption (the TBABS model; Wilms et al. 2000). We extrapolated the best-fitting model for each observation to cover the PCA energy range and then used the PCA response matrix to convert this to an equivalent PCA count rate. The resulting PCA-equivalent count rates are shown on Fig. 3.

3 ANALYSIS AND RESULTS

3.1 The Model

If radiative efficiency is a power-law function of the central mass accretion rate, $\eta \propto \dot{M}^{\beta}$, and the mass accretion rate follows an exponential decay with e-folding time $\tau_{\rm m}$, the X-ray luminosity should follow $L_{\rm X} = A\exp(-t(1+\beta)/\tau_{\rm m})$. We therefore fit a simple model $L_{\rm X} = A\exp(-t/\tau) + C$ to decaying intervals of the light curves to estimate the decay time-scales during soft-state and hard-state intervals to give luminosity decay timescales $\tau_{\rm s}$ and $\tau_{\rm h}$, respectively. The constant C accounts for any constant light from contaminating background sources.

Assuming the radiative efficiency is constant at high luminosities ($\beta = 0$ in the soft state), the luminosity decay in the soft state should track the decay in $\dot{M}$, i.e. $\tau_{\rm s} = \tau_{\rm m}$. But if the radiative efficiency scales with accretion rate ($\beta > 0$) in the hard state, the X-ray luminosity will have a different e-folding time, $\tau_{\rm h} = \tau_{\rm m}/(1+\beta)$. We can then estimate β by comparing the decay times in soft and hard states as $\beta = \tau_{\rm s}/\tau_{\rm h} - 1$. If there is no change in radiative efficiency, we expect $\beta = 0$, while if there is a change to $\eta \propto \dot{M}$ regime we should see $\beta = 1$.

3.2 Results

We have studied the final weeks of all the outbursts listed in Table 2. Based on an initial, visual inspection of the light curves, for each source we identified two regions of decay separated by the soft–hard state transition. (During this transition – spanning intermediate states – the light curve often stays approximately constant or even rises slightly). The model above was fitted[1] to each of these regions to give estimates of $\tau_{\rm s}$ and $\tau_{\rm h}$. These are given in Table 1 and the data and models are plotted in the Appendix. All light curves are in the 3-20 keV band.

The clearest example of exponential decay comes from the well-observed 2005 outburst of GRO J1655−40 shown in Fig. 2. There are two distinct periods of exponential decay, ignoring the intermediate state where there is a small rise in count rate. Fitting these gave $\tau_{\rm s}$ and $\tau_{\rm h}$ values of 13.85 ± 0.15 and 6.72 ± 0.08 d, respectively. The decay rate almost exactly doubled following the transition into the hard state, giving $\beta = 1.06 \pm 0.02$. (Only the *RXTE* data were fitted; the *Swift* data were used only to verify the extrapolation of the source *RXTE* light curve to low fluxes.)

The other sources show more varied results with β value ranging from -0.1 to 2.90. In some cases it was not possible to clearly identify suitable decaying intervals. For some outbursts any period of exponential decay was very short, for some others it was too sparsely sampled (e.g. XTE J1650−500). Even where there are sufficient data, in many cases the residuals for the exponential model fits show systematic structure: deviations from a single, unbroken exponential decay within a particular state.

In order to focus on a single period of exponential decay with a constant decay rate, we used a different fitting strategy. Specifically, we calculated 'local' τ values for each point by fitting only that point and the next four. We then find the modal τ and identify the longest interval in the light curve consistent with this decay rate (dominated by τ values within 1 d of the mode). New values of $\tau_{\rm s}$, $\tau_{\rm h}$ and β were then estimated by fitting over these smaller intervals of consistent decay rate. Furthermore, we ignore intervals containing fewer than eigth consecutive points. Table 2 shows the results. The appendix shows the results of the fitting and provides notes on individual outbursts. This more conservative analysis yielded five β estimates; with the exception of GX $339-4$ these lie in the range 1.0 ± 0.3.

[1] The fitting was performed by minimizing the usual χ^2 fit statistic.

System name (1)	Outburst (2)	No. of obs. (3)	$\tau_{\rm s}$ (d) (4)	Decay length (5)	$\tau_{\rm h}$ (d) (6)	Decay length (7)	β (8)
GRO J1655−40	2005	495	14.02 ± 0.13	50	6.85 ± 0.05	73	1.05 ± 0.01
XTE J1550−564	1998	234	8.97 ± 0.14	21	2.33 ± 0.05	9	2.85 ± 0.07
	1999	66	14.80 ± 1.11	8	6.87 ± 0.03	70	1.15 ± 0.09
XTE J1650−500	2001	106	16.18 ± 0.25	21	–	–	–
GX 339−4	2002	174	16.28 ± 0.28	13	18.21 ± 0.13	37	-0.11 ± 0.01
	2004	251	17.09 ± 1.29	4	14.15 ± 0.07	56	0.21 ± 0.02
	2007	244	16.94 ± 0.34	13	7.43 ± 0.32	28	1.28 ± 0.06
	2010	294	–	–	11.46 ± 0.28	19	–
4U 1543−475	2002	102	6.10 ± 0.15	12	4.97 ± 0.04	54	0.23 ± 0.01
H 1743−322	2003	219	14.06 ± 0.37	11	4.81 ± 0.07	40	1.92 ± 0.06
	2004	49	22.06 ± 0.82	7	5.66 ± 0.14	18	2.90 ± 0.13
	2005	23	12.92 ± 1.28	4	5.49 ± 0.12	10	1.35 ± 0.14
	2009	49	20.07 ± 1.68	9	8.02 ± 0.17	16	1.50 ± 0.13
	2010	58	16.92 ± 0.86	10	6.95 ± 0.11	23	1.43 ± 0.08
	2011	39	11.75 ± 0.52	8	7.39 ± 0.15	17	0.59 ± 0.03

Table 1. Details of the outbursts used in our sample. Column 1 gives the source name, column 2 gives the year of each outburst and column 3 gives the total number of *RXTE* observations used. Columns 4 and 6 show the e-folding times, columns 5 and 7 show the number of observations included in the fit, and column 8 shows the β values. Missing values indicate light curves with insufficient data to properly fit exponential curves.

System name (1)	Outburst (2)	$\tau_{\rm s}$ (d) (3)	Decay length (4)	$\tau_{\rm h}$ (d) (5)	Decay length (6)	β (7)
GRO J1655−40	2005	13.85 ± 0.15	40	6.72 ± 0.08	48	1.06 ± 0.02
XTE J1550−564	1998	9.76 ± 0.26	15	–	7	–
	1999	14.80 ± 1.11	8	6.95 ± 0.08	22	1.13 ± 0.09
XTE J1650−500	2001	16.12 ± 0.27	20	–	–	–
GX 339−4	2002	12.04 ± 0.45	8	8.46 ± 1.24	9	0.42 ± 0.06
	2004	–	4	8.78 ± 0.70	21	–
	2007	–	7	8.87 ± 1.32	16	–
	2010	–	–	5.88 ± 0.68	8	–
4U 1543−475	2002	6.10 ± 0.15	12	2.70 ± 0.08	12	1.26 ± 0.05
H 1743−322	2003	12.96 ± 0.51	8	7.41 ± 0.91	14	0.75 ± 0.10
	2004	–	6	5.19 ± 0.27	13	–
	2005	–	6	–	6	–
	2009	–	7	–	6	–
	2010	–	6	10.69 ± 2.40	10	–
	2011	–	–	–	7	–

Table 2. The same parameters as in Table 1 after fitting only restricted sections of the light curves (see the text for details).

4 DISCUSSION

We have examined the decaying stages in the X-ray light curves of 15 outbursts of six BH X-ray binaries. We found that in all cases the last few weeks of each outburst can be described in terms of nearly exponential decays. For the seven outbursts with well-observed exponential decays in the soft state, the mean e-folding time is 12 ± 1 d, while for the ten outbursts with well observed exponential decays in the hard state, the mean e-folding time is 7 ± 1 d (see Table 2). Several outbursts (e.g. of GX 339−4) show more complicated behaviour, sometimes with little or no obvious decay during the soft state. As such, it is difficult to say whether the models discussed above will apply to all BH LMXB systems/outbursts or just a subset. Homan et al. (2005) previously noted the factor 2 change in decay time-scale in their early analysis of the 2005 outburst of GRO J1655−40. Here, we have confirmed their results for that one outburst and showed that similar behaviour can be seen in the other four outbursts with well-constrained exponential decays in both states.

We characterized the change in the decays during soft and hard states using a parameter $\beta = \tau_{\rm s}/\tau_{\rm h} - 1$. Assuming constant η in the soft state, such that $\tau_{\rm s} = \tau_{\rm m}$ (the decay of $\dot{M}$), this parameter can be interpreted as the index of the efficiency scaling: $\eta \propto \dot{M}^{\beta}$. Of the five systems with the most reliable β estimates, four show $\beta \approx 1$, while GX 339−4 shows $\beta \approx 0.4$.

We estimated the decay rates using broad-band light curves (3-20 keV) from the *RXTE* PCA. Such a dramatic change in the decay rate is not an artifact of spectral evolution: within each of the soft and hard states, the spectral evolution is relatively modest (see Fig.1). We conclude that there is a genuine change in the speed at which the X-ray luminosity drops. If $L_{\rm X} = \eta \dot{M} c^2$, then either the decay rate of $\dot{M}$ changes around the state transition or η decreases with time (and luminosity) after the state transition.

The change in the decay could signal the switch from a disc-dominated, radiatively efficient soft state to a radiatively inefficient mode of accretion (such as an ADAF or JDAF type flow) in the hard state. As discussed above, such a model – in which the soft state has η constant with $\dot{M}$, but the hard state is governed by an accretion flow that becomes radiatively inefficient at low $\dot{M}$ ac-

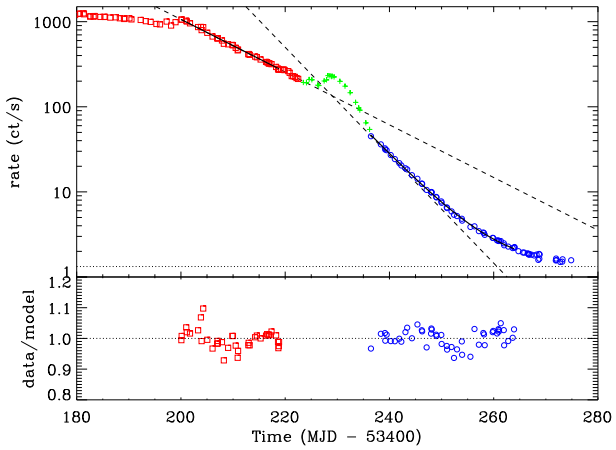

Figure 2. The decay of the 2005 outburst of GRO J1655−40, fitted with separate exponential decay models in the soft state (square red points) and hard state (circular blue points). An additional constant is included in the hard-state model to account for the saturation at low fluxes (caused by background contamination). The dashed lines show the exponential decays extrapolated over the full decay region. The bottom panel shows the data/model residuals.

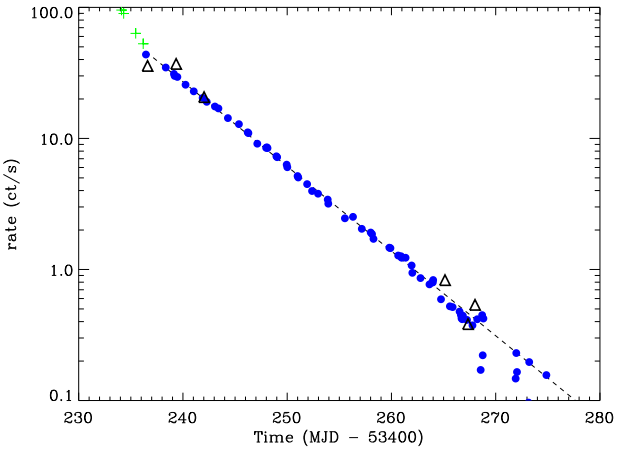

Figure 3. Close-up of the hard state decay of the 2005 outburst of GRO J1655−40 after subtracting the constant (as fitted in Fig. 2). The black triangular points show the *Swift* data, which agree with the *RXTE* data after the constant has been subtracted.

cording to $\eta \propto \dot{M}$ – matches the results. This interpretation is consistent with other studies comparing radio and X-ray luminosities over a sample of binaries (Fender et al. 2003; Merloni et al. 2003). By contrast, Knevitt et al. (2014) required a steeper efficiency scaling (with $\beta > 3$) to explain the lack of known short period BH LMXBs relative to NS LMXBs. Reconciling these results – the factor ≈ 2 change in the decay slopes implying $\eta \propto \dot{M}$ scaling, and the lack of short period BH LMXBs – would require either that there is another explanation for the absence of short-period BH systems, or that the efficiency scaling becomes much steeper at lower luminosities, below those accessible with the *RXTE* data.

It is the average radiative efficiency (averaged over any contributing spectral components) that is required to change. There could be two emission components with radiative efficiencies that are very different, but each is constant with time. The observed faster decay in the hard state could be produced if the source emission evolves from being dominated by the more radiatively efficient component to being dominated by the least radiatively efficient component, so that the weighted average of the radiative efficiency drop with $L_{\rm X}$. But such a model requires fine-tuning to explain the observed results. Consider two emission processes with spectra $S_1(E)$ and $S_2(E)$, and radiative efficiencies η_1 and η_2 (with $\eta_2 < \eta_1$). The mass accretion rate $\dot{M}$ powering the source is divided such that a fraction a drives the first component and $(1-a)$ drives the second. The total luminosity is $L \propto \dot{M}(\eta_1 a S_1 + \eta_2(1-a)S_2)$. The term in brackets is the emission-averaged radiative efficiency. In order to reproduce the doubling in decay rate, a would have to be a function of $\dot{M}$ in the hard state in such a way to make the emission-averaged radiative efficiency scale linearly with $\dot{M}$, which seems contrived. Further, the relatively modest evolution of the spectrum during the hard-state decay does not support such a model unless the two components have very similar spectra over the observed X-ray band.

The above interpretation assumes that the mass accretion rate decays as $\dot{M} \propto \exp(-t/\tau_{\rm m})$ through most of the outburst decay, and in particular, $\tau_{\rm m}$ does not change around the state transition. An alternative explanation is that η is constant and there is a change in $\tau_{\rm m}$ coincident with the state transition. The coincidence in time would require that the state transition and the change in the decay rate of $\dot{M}$ are causally linked (either one causes the other or they are both triggered by some other event) by some mechanism not included in the current models of disc outbursts (van Paradijs 1996; King & Ritter 1998; Dubus et al. 2001; Lasota 2001)

We conclude that the most plausible explanation is in terms of a change in the radiative efficiency, and that the soft- to hard-state transition is the result of the inner accretion flow transforming from a standard, efficient accretion disc to a radiatively inefficient flow as suggested by models such as Narayan & Yi (1995) and Esin et al. (1997).

ACKNOWLEDGEMENTS

AJE is supported by an STFC studentship. SV and GAW acknowledge support from STFC consolidated grant ST/K001000/1. This research has made use of NASA's Astrophysics Data System and of data, software and web tools obtained from NASA's HEASARC, a service of Goddard Space Flight Center and the Smithsonian Astrophysical Observatory. We thank an anonymous referee for a careful reading of the paper and a constructive report.

REFERENCES

Arnaud K. A., 1996, in ASP Conf. Ser., Vol. 101, Astronomical Data Analysis Software and Systems V., Jacoby G. H., Barnes J., eds., Astron. Soc. Pac., San Fransisco, p. 17
Belloni T., Homan J., Casella P., van der Klis M., Nespoli E., Lewin W. H. G., Miller J. M., Méndez M., 2005, A&A, 440, 207
Belloni T. M., 2010, in Lecture Notes in Physics, Vol. 794, The Jet Paradigm. Springer-Verlag, Belloni T., ed., Berlin, p. 53
Chen W., Shrader C. R., Livio M., 1997, ApJ, 491, 312
Coriat M. et al., 2011, MNRAS, 414, 677
Done C., Gierlinski M., Kubota A., 2007, A&AR, 15, 1
Dove J. B., Wilms J., Begelman M. C., 1997, ApJ, 487, 747

Dubus G., Hameury J.-M., Lasota J.-P., 2001, A&A, 373, 251
Esin A. A., McClintock J. E., Narayan R., 1997, ApJ, 489, 865
Falcke H., Körding E., Markoff S., 2004, A&A, 414, 895
Fender R., Gallo E., 2014, Space Sci. Rev., 183
Fender R., Homan J., Belloni T. M., 2009, MNRAS, 396, 1370
Fender R. P., Gallo E., Jonker P. G., 2003, MNRAS, 343, L99
Haardt F., Maraschi L., 1993, ApJ, 413, 507
Homan J., Belloni T., 2005, Ap&SS, 300, 107
Homan J., Kong A., Tomsick J., Miller J., Campana S., Wijnands R., Belloni T., Lewin W., 2005, ATel, 644
Jonker P. G. et al., 2010, MNRAS, 401, 1255
King A. R., Ritter H., 1998, MNRAS, 293, L42
Knevitt G., Wynn G. A., Vaughan S., Watson M. G., 2014, MNRAS, 437, 3087
Körding E. G., Fender R. P., Migliari S., 2006, MNRAS, 369, 1451
Kuulkers E., 1998, New Astron. Rev., 42, 1
Lasota J.-P., 2001, New Astron. Rev., 45, 449
Markoff S., Falcke H., Fender R., 2001, A&A, 372, L25
Markoff S., Nowak M. A., Wilms J., 2005, ApJ, 635, 1203
McClintock J. E., Remillard R. A., 2006, In Compact Stellar X-Ray Sources, Lewin W., van der Klis M., eds., Cambridge Univ. Press, Cambridge, p. 157
Merloni A., Heinz S., di Matteo T., 2003, MNRAS, 345, 1057
Miller-Jones J. C. A., Jonker P. G., Maccarone T. J., Nelemans G., Calvelo D. E., 2011, ApJL, 739, L18
Motta S., Homan J., Munoz-Darias T., Casella P., Belloni T. M., Hiemstra B., Mendez M., 2012, MNRAS, 427, 595
Narayan R., Yi I., 1995, ApJ, 452, 710
Plotkin R. M., Gallo E., Jonker P. G., 2013, ApJ, 773, 59
Poutanen J., 1998, in Theory of Black Hole Accretion Disks, Abramowicz M. A., Bjornsson G., Pringle J. E., eds., Cambridge Univ. Press, Cambridge, p. 100
Remillard R. A., McClintock J. E., 2006, ARA&A, 44, 49
Reynolds M. T., Reis R. C., Miller J. M., Cackett E. M., Degenaar N., 2014, MNRAS, 441, 3656
Shakura N. I., Sunyaev R. A., 1973, A&A, 24, 337
Stiele H., Muñoz-Darias T., Motta S., Belloni T. M., 2012, MNRAS, 422, 679
Tomsick J. A., Yamaoka K., Corbel S., Kalemci E., Migliari S., Kaaret P., 2014, ApJ, 791
van der Klis M., 2006, Rapid X-ray Variability, Lewin W. H. G., van der Klis M., eds., Cambridge Univ. Press, Cambridge
van Paradijs J., 1996, ApJL, 464, L139
Wilms J., Allen A., McCray R., 2000, ApJ, 542, 914

This paper has been typeset from a TEX/ LATEX file prepared by the author.

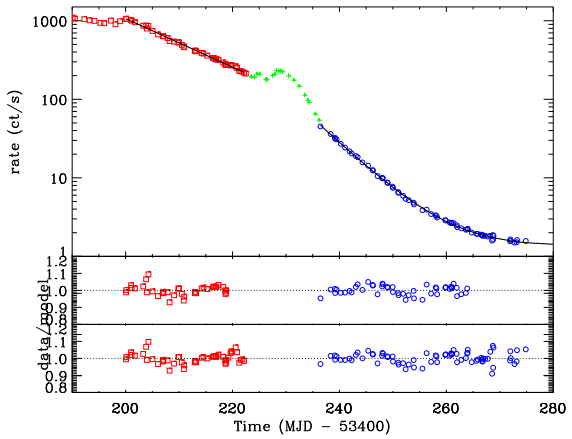

Figure A1. The decaying stages of the 2005 outburst of GRO J1655−40. The top panel shows the 3-20 keV light curve with exponential decay models (black) fitted to both soft-state (red squares) and hard-state (blue circles) data. The bottom panel shows the residuals from the fit described in Table 1, the middle panel shows the results from the fit described in Table 2, using only intervals of nearly uniform decay. (A constant component was added to the model as described in the text.)

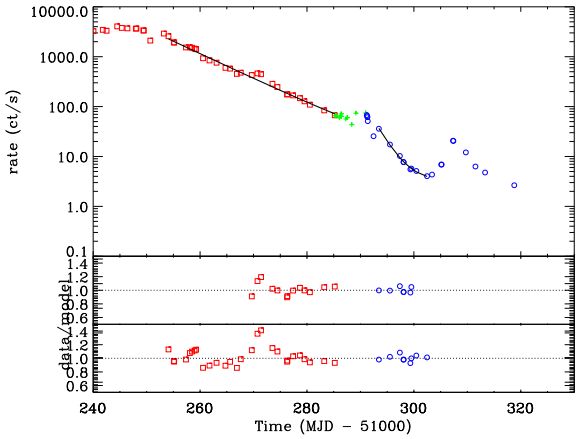

Figure A2. The decaying stages of the 1998 outburst of XTE J1550−564. The soft-state has a more complicated decay that is not a single exponential decay due to the flare around MJD 51270. The hard state itself is also affected by a flare, this time dominating the whole decay, leaving only a small section that could be fit.

APPENDIX A: ADDITIONAL PLOTS

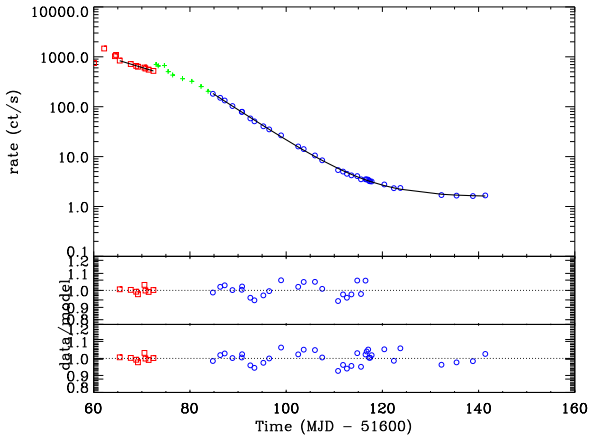

Figure A3. The decaying stages of the 1999 outburst of XTE J1550−564.

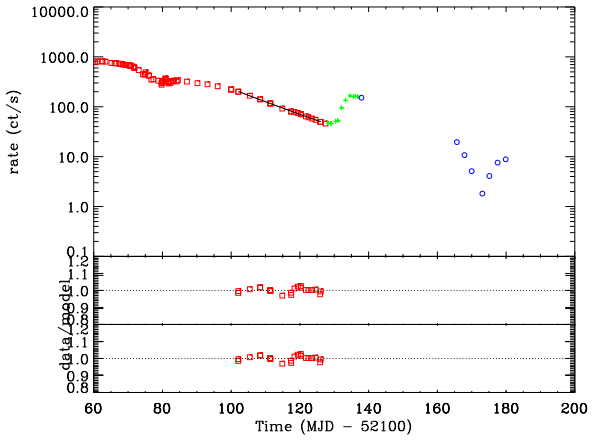

Figure A4. The decaying stages of the 1999 outburst of XTE J1650−500.

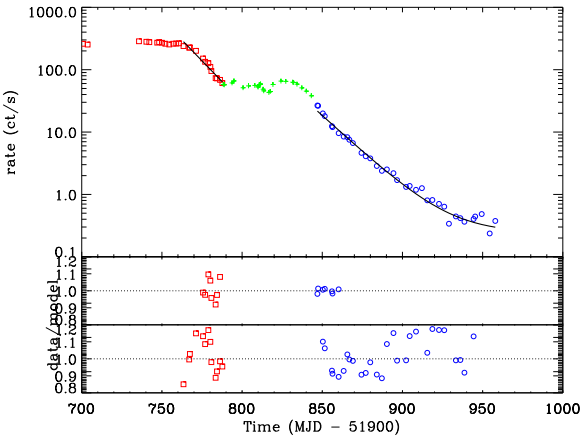

Figure A5. The decaying stages of the 2002 outburst of GX 339−4. We have β for this outburst, however there are certain features of the GX 339−4 outbursts that should be noted. Compared to the overall length of the soft state, the soft decaying interval is very short, with the source staying at near constant luminosity for many weeks.

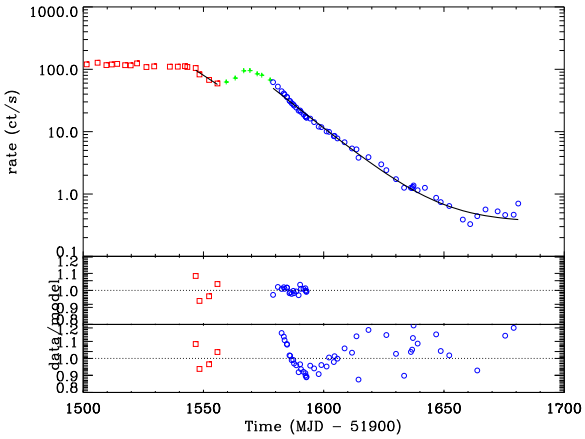

Figure A6. The decaying stages of the 2004 outburst of GX 339−4. The soft-state decay only lasts for around a week, making it too short to reliably measure its properties.

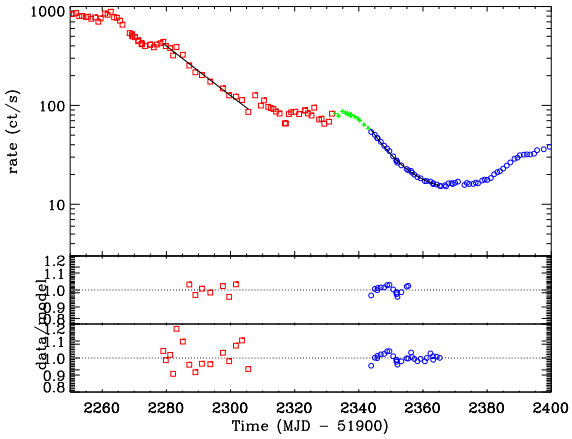

Figure A7. The decaying stages of the 2007 outburst of GX 339−4.

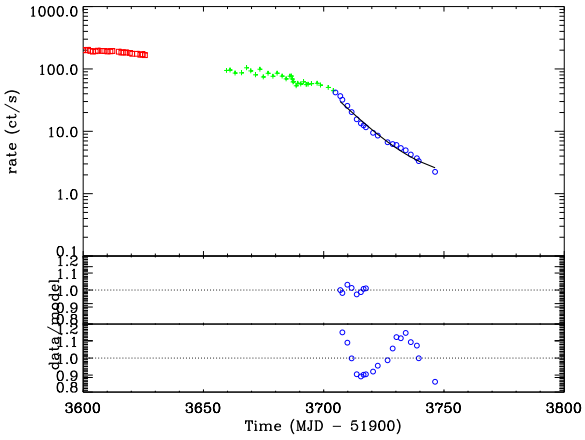

Figure A8. The decaying stages of the 2010 outburst of GX 339−4.

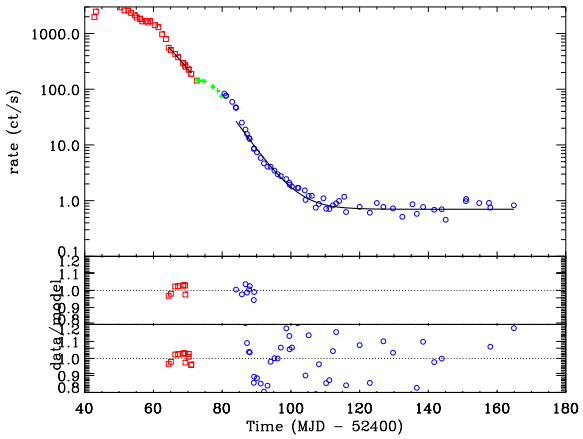

Figure A9. The decaying stages of the 2002 outburst of 4U 1543−475.

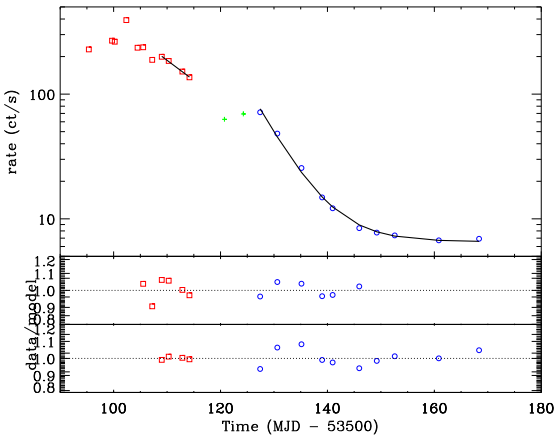

Figure A12. The decaying stages of the 2005 outburst of H 1743−322.

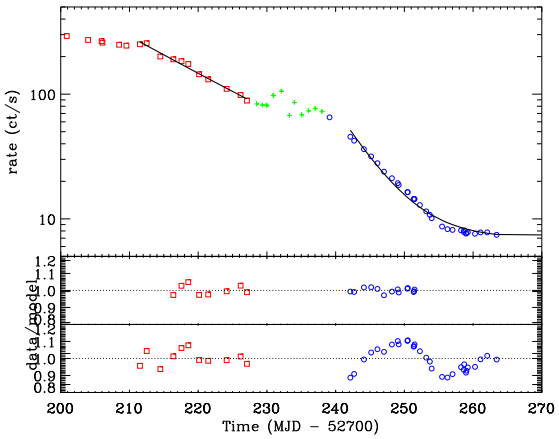

Figure A10. The decaying stages of the 2003 outburst of H 1743−322.

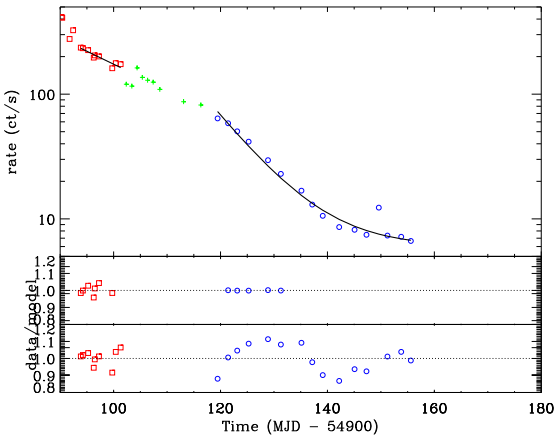

Figure A13. The decaying stages of the 2009 outburst of H 1743−322.

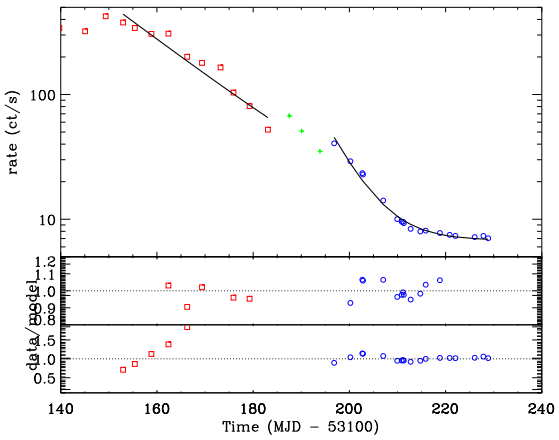

Figure A11. The decaying stages of the 2004 outburst of H 1743−322.

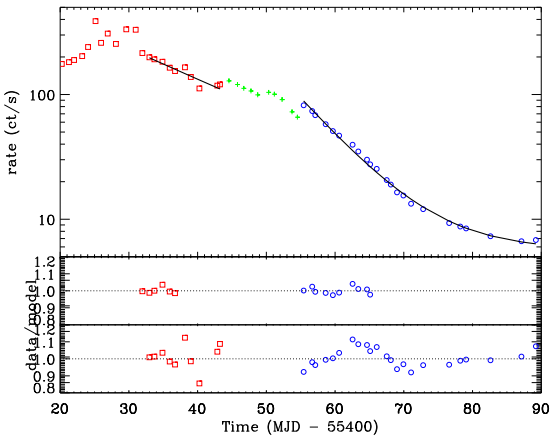

Figure A14. The decaying stages of the 2010 outburst of H 1743−322.

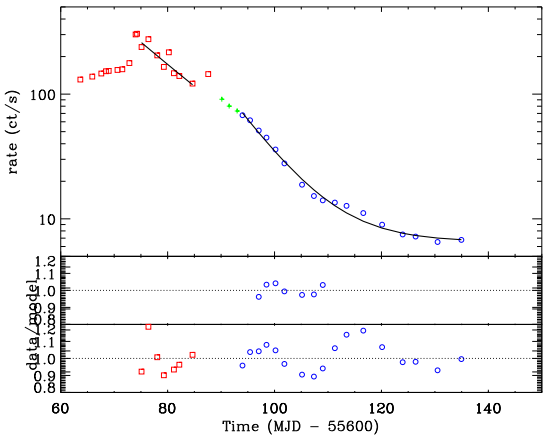

Figure A15. The decaying stages of the 2011 outburst of H 1743−322.